SPECIAL TOPIC — Physical research in liquid crystal

Asymmetric dynamic phase holographic grating in nematic liquid crystal*

Chang-Yu Ren(任常愚)[1,†], Hong-Xin Shi(石宏新)[1], Yan-Bao Ai(艾延宝)[2], Xiang-Bao Yin(尹向宝)[1], Feng Wang(王丰)[1], and Hong-Wei Ding(丁红伟)[1]

[1] School of Science, Heilongjiang University of Science and Technology, Harbin 150022, China
[2] Electrization and Control Engineering School, Heilongjiang University of Science and Technology, Harbin 150022, China

(Received 27 May 2016; published online 2 August 2016)

A new scheme for recording a dynamic phase grating with an asymmetric profile in C_{60}-doped homeotropically aligned nematic liquid crystal (NLC) was presented. An oblique incidence beam was used to record the thin asymmetric dynamic phase holographic grating. The diffraction efficiency we achieved is more than 40%, exceeding the theoretical limit for symmetric profile gratings. Both facts can be explained by assuming that a grating with an asymmetric saw-tooth profile is formed in the NLC. Finally, physical mechanism and mathematical model for characterizing the asymmetric phase holographic grating were presented, based on the photo-refractive-like (PR-like) effect.

Keywords: nematic liquid crystal, asymmetric phase grating, diffraction efficiency, photorefractive effect

PACS: 42.70.Df, 42.65.Hw, 42.40.Eq, 42.40.Lx **DOI:** 10.1088/1674-1056/25/9/094218

1. Introduction

Electro–optical properties of the liquid crystals (LCs), such as the reorientation of LC molecules (Photorefractive Effect, PRE) with external electric fields, make these materials one kind of the most important media for recording static and dynamic holograms (DHs). The investigations of thin phase dynamic gratings in liquid crystal (LC) have been concentrated mainly on their diffraction characteristics. The thin phase dynamic gratings have shown great promise in applications of optical communication and optical information processing. They also solve the problem of dynamic holographic correction of distortions.[1–5]

Thin dynamic holograms formed in an LC layer are free of limitations imposed by angular and spectral selectivities and, therefore, can be used in wide fields of view and a wide spectral range. However, according to the traditional understanding of the mechanism of dynamic grating formation in LC, the fringe of such grating has to have symmetrical profiles. It is well known that the diffraction efficiency (DE) of these thin phase holographic gratings to the $+1$st and -1st orders of diffraction cannot exceed 25%, 33.8%, and 40.5% for triangle, sinusoidal, and square thin phase gratings, respectively.[6] The limitation of DE value of this hologram is a significant disadvantage when it is used as a corrector

To solve this problem, a new efficient approach was proposed and implemented to fabricate the thin dynamic holographic grating with an asymmetric fringe profile, such as a saw-tooth holographic grating (it cannot be expressed as an even function). It is well known that such grating, which still preserves their thin nature, can provide very high values of DE, up to 100% to one of the first orders. It would be expected that the diffraction efficiency is asymmetric relative to the angle of incidence.[7–10]

In this paper, we propose a new efficient approach to record the thin dynamic phase grating (refractive index grating) with an asymmetric fringe profile in the LC cell. The first-order DE exceeds the theoretical limit for symmetric profile gratings. This asymmetric grating has a significant asymmetric diffraction pattern, which is accompanied by the transfer of energy from one beam to another. We also investigate the asymmetric grating formation mechanism and present a new mathematical model of the asymmetric grating. The conjecture that the function almost perfectly fits a saw-tooth profile is established.

Based on our experimental results, we believe that the surface-mediated PR mechanism plays a dominant role in the grating recording, and the Carr–Helfrich effect in the bulk may have a significant contribution in amplifying the diffraction of hidden grating.

2. Experiments

The investigated liquid-crystal cell which had a sandwich-like structure consisted of a liquid-crystal (LC) layer and photoconductor (PC) layers to which a certain dc voltage was applied. The fabrication process of making such samples used in our experiments was 4-cyano-4′-pentyl-biphenyl (5CB, Aldrich Ltd.) doped with fullerene C_{60} (C_{60}, 99.9%). Fullerene C_{60} is an efficient photo charge generator The doping of the fullerene in LC enhanced photoconductivity and the

*Project supported by the Science and Technology Programs of the Educational Committee of Heilongjiang Province, China (Grant No. 12541730) and the National Natural Science Foundation of China (Grant No. 61405057).

†Corresponding author. E-mail: renchangyu@126.comedu.cn; renchangyu@usth.edu.cn

© 2016 Chinese Physical Society and IOP Publishing Ltd

resulting nonlinearity of LC led to an increase in diffraction efficiency. The dopant concentration used in these studies was 0.05% by weight. The typical absorption constants of these samples varied from 5 cm^{-1} to 10 cm^{-1}, depending on the concentration. The glass substrates were coated with a transparent electrode of indium tin oxide (ITO) for the application of an external dc voltage. The primary homotopic alignment of NLC molecules was provided by the treatment of the ITO-coated cell windows with the surfactant hexadecyltrimethyl ammonium bromide (HTAB). The liquid crystal cell was prepared by assembling two ITO glasses, with a gap of 20 μm, set by Mylar spacers. The cells were filled by capillary action in the isotropic phase at an elevated temperature (60 °C) and slowly cooled down to room temperature.

The experimental setup was a standard two-beam coupling (2BC) arrangement as shown in Fig. 1. Diffraction grating was recorded by the radiation of an He–Ne laser (633 nm), which was split into two p-polarized mutually coherent lights. The interference pattern was generated by these two plain waves of equal intensity. Readingout of the thus recorded hologram was done using one writing beam. The sample was set perpendicular to the beam intersection plane and could be rotated in the plane of the beam incidence (Fig. 1). The sample was tilted at an angle of $\beta = 45°$ with respect to the bisector of the two writing beams. The crossing angle α between the two writing beams was set at 1.5°. The beam diameter D was 2.0 mm at the intersection on the sample. These two p-polarized writing beams intersected inside the cell and produced an intensity distribution of the interference fringes, resulting in the recording of dynamic holographic grating (hologram). A dc voltage of 0–5 V was applied to the cell. The intensity of diffraction to the nth diffraction order was registered by photoelectric means. The ambient temperature was controlled at 23–30 °C.

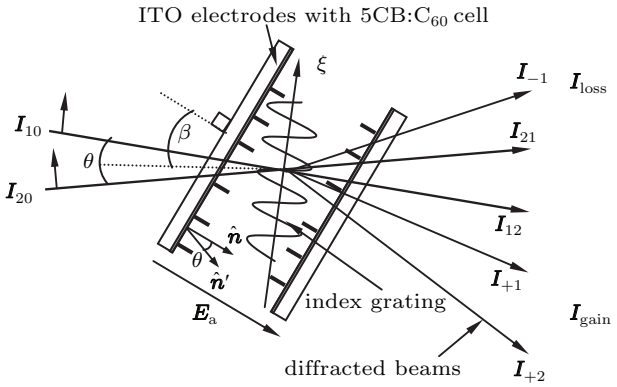


Fig. 1. Schematic diagram of two-beam coupling.

The experiments were carried out as follows: First, the holographic grating (hologram) was recorded in the film with an applied dc voltage of 1.5 V. Then, the writing beams and the applied dc voltage were switched off simultaneously. At last, the reference beam (as probe beam) and a high voltage, greater than the voltage used during the recording process, were turned on at the same time. Then an asymmetric diffraction pattern with strong diffraction efficiency was observed.

3. Results and discussion

A typical diffraction pattern observed is shown in Fig. 2. Under the optimal experimental conditions, two p-polarized coherent writing beams with equal power (633 nm, $I_{10} = I_{20} =$ 4.7 mW, beam diameter: 2 mm) were overlapped on the LC cell at a small wave-mixing angle in the air ($\alpha \approx 1.5°$). The corresponding optical intensity grating spacing is $\Lambda \approx 29$ μm. In our studies the dimensionless parameter $Q = 2\pi\lambda L/n\Lambda^2 \approx 0.07 \ll 1$, where λ is the wavelength of writing beams, L is the thickness of grating, which is the optical path length through the sample, and n is the average refractive index of the medium. It indicates that the grating is working in the Raman–Nath regime, and the angular spread of the wavevector is much larger than Bragg angle. Consequently, multi-order self-diffractions were allowed n two-beam coupling experiments. Strong asymmetric diffraction beams of more than the 7th order were observed in our experiments.



Fig. 2. (color online) Asymmetric diffraction pattern of grating in TBC experiment under the application of a dc voltage of 2.5 V.

If the writing beams are s-polarized or no dc voltage is applied on the cells, no diffraction is observed; if the writing beams are p-polarized, the asymmetric diffraction appears, and the transfer of energy between the beams occurs. The polarization dependence and the requirement of a dc electric field are powerful evidence that the grating originates from the PR effect Thermal effect, other phase change, and order-disorder transitions are ruled out as possible mechanisms.

The photograph of Fig. 3 shows the dependence of the revealed asymmetric diffraction pattern on the increase of the applied dc voltage. When the applied dc voltage is less than 1.0 V, the self-diffraction phenomenon cannot be observed and only two transmitted beam spots were observed. When the applied dc voltage is up to 1.5 V, we begin to observe the self-diffraction phenomenon. With the increase of the applied dc voltage, higher-order, up to 12 diffraction orders, asymmetric diffraction spots are observed. Continuing to increase the applied dc voltage (up to 3.5 V) we will see diffraction order reduction When the applied dc voltage is greater than 3.5 V, strong dynamic scattering and background noise become obvious, as shown in Figs. 3(e) and 3(f) We surmise that the honeycomb-like domain might be formed. For safety considerations, the maximum value of applied dc voltage used in our experiments is 3.5 V. We find that the dynamic scattering and background noise level might be suppressed when the ambient temperature falls below 23 °C (5CB phase transition temperature).

An asymmetric diffracted light intensity distribution curve can be obtained easily by using Origin graphics software as shown in Fig. 4. The intensity distribution curve is normalized. We can obviously see the asymmetry of the diffracted

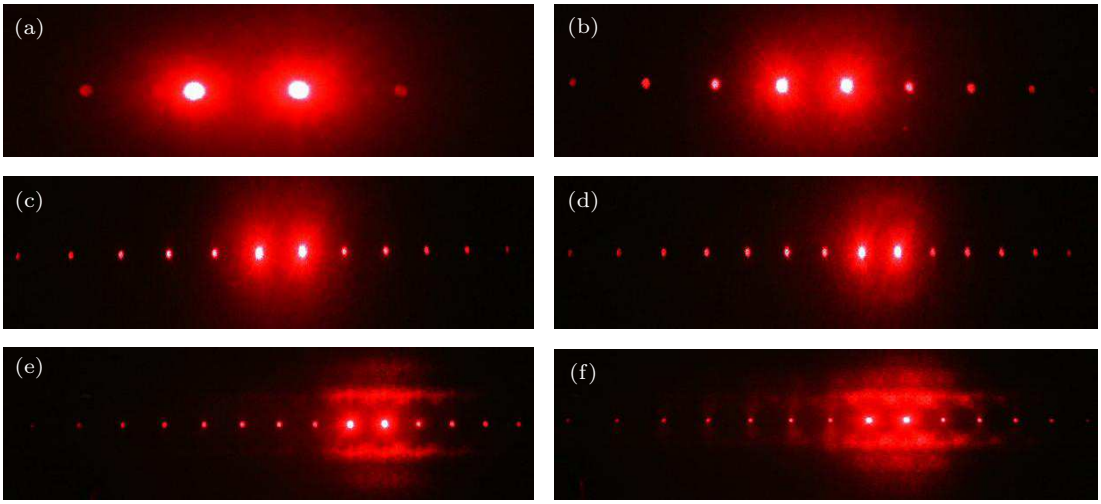


Fig. 3. (color online) Diffracted patterns in the presence of applied dc voltages (a) 1.0 V, (b) 1.5 V, (c) 2.0 V, (d) 2.5 V, (e) 3.5 V, (f) 4.0 V.

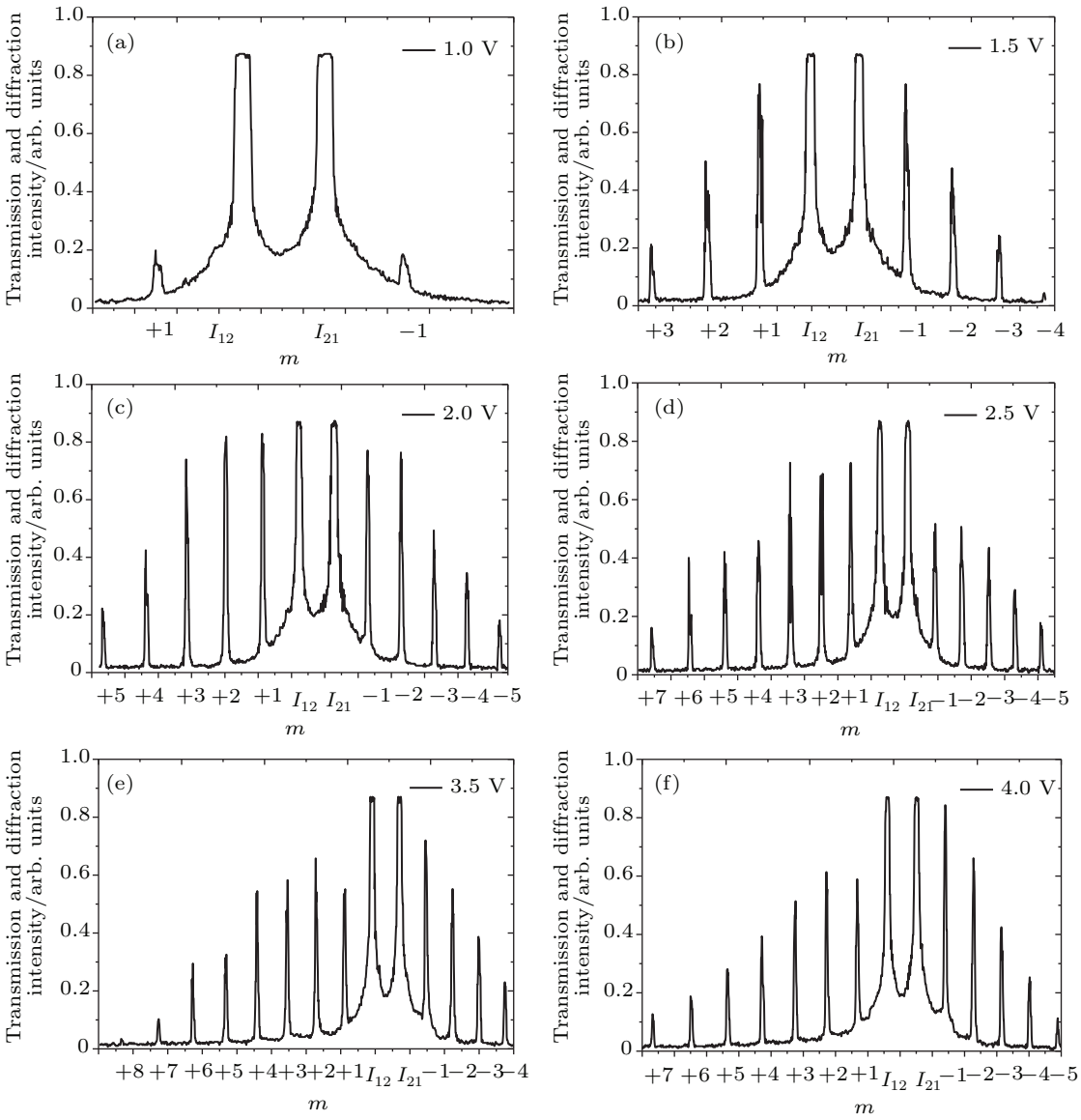


Fig. 4. Dynamics of the diffraction intensity of all the orders at different applied dc voltages: (a) 1.0 V, (b) 1.5 V, (c) 2.0 V, (d) 2.5 V, (e) 3.5 V, and (f) 4.0 V.

light intensity profiles. Diffraction intensity distribution has the following characteristics: (I) When the dc voltage is small, the transmitted light intensity on both sides of the diffracted light exhibits substantially symmetrical distribution; (II) When the dc voltage is increased to 2.0 V, the diffracted light intensity on both sides exhibits an asymmetric phenomenon. With the dc voltage increasing, the appearance of new diffraction orders and the asymmetric diffraction distribution are significantly enhanced.

In addition, we investigate the first-order diffracted beam diffraction efficiency dependence on the applied dc voltage The experimental setup for recording and reconstruction of the dynamic grating is shown in Fig. 1.

The first-order diffraction efficiency is conventionally defined as an intensity ratio of the first-order diffraction beam to the incident beam in the absence of one side of the two beams and can be written as

$$\eta_1\,(\%) = \left(\frac{I_{\pm 1}}{I}\right) \times 100\%. \tag{1}$$

The dependencies of the diffraction efficiency of the firstorder diffracted beam on the externally applied dc electric fields are shown in Fig. 5. The first-order diffraction efficiency rises significantly when the applied dc voltage exceeds 1.5 V. It shows that the diffraction efficiency increases until a maximum DE is reached at a certain voltage and then decreases for a further increase of the applied dc voltage. The maximum value of the first-order diffraction efficiency measured is up to 40% and occurred the voltage is around 2.6 V. It exceeds the theoretical limit of 34% predicted by the Raman-Nath theory for a symmetrical grating. Our experiments show that, the higher the voltage is, the larger the DE is, in the reading process. We demonstrate that a high dc electric field could enhance the diffraction efficiency of the grating during the reconstruction process. Further increasing of the voltage will diminish the reorientation and induce a strong dynamic scattering that results in the decrease of the diffraction efficiency.

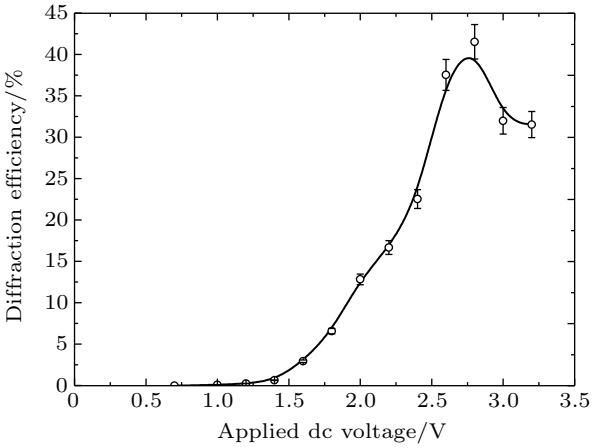


Fig. 5. Voltage dependence of the first-order diffraction efficiency on the applied voltage.

The maximum DE value obtained in our experiments amounts to 40%, exceeding the theoretical limit for a thin phase hologram with a symmetric line profile. The only reason for the side effect can be the grating asymmetry. The multi-order asymmetric distribution of the diffraction light indicates that the asymmetric grating remains thin. Diffraction efficiency enhancement is strongly affected by the applied dc voltage indicating that the asymmetric grating is formed near the interface (between the alignment layer and the NLC).

The mechanisms of the photorefractive effect in homeotropic alignment NLC were proposed earlier.[11–15] Two types of space-charge fields, generated in the NLC cell should be considered to explain the PR effect. The first type is the bulk space-charge fields consisting of the usual photo-refractive-like space-charge field initiated by light-induced charge photogeneration and redistribution, and the field-dependent space-charge fields that arise from the Carr–Helfrich effect due to the conductivity and the dielectric anisotropies. The second type is the surface-charge induced electric field attributed to the modulation of the charge distribution near the interface.

These space-charge fields, combined with applied dc field, create volume torques that drive bulk reorientation of the LC director. The surface-charge field also causes a surface torque owing to the modulation of the surface anchoring. These surface-charge field profiles are asymmetrical. As a result, an asymmetric refractive index grating profile is induced by these space-charge fields. The asymmetry of the surface electric field on the surface of the aligning surfaces may play a crucial role in the formation of the asymmetric grating.

Taking into account of the significant difference between the DE to the 1st diffraction order and an asymmetric diffracted light intensity distribution, the only reason may be the grating with an asymmetry profile. In order to elucidate the asymmetrization of the phase grating profile, we present a simple model to qualitatively explain the asymmetric grating.

We assume that the liquid crystal is illuminated with a sinusoidally modulated light of intensity $I(x) \sim I_{\rm o}(1 + m\cos q\xi)$,[11–13] where m is the optical intensity modulation factor, $q = 2\pi/\Lambda$ is the magnitude of the grating vector, and Λ is the grating spacing, ξ is the coordinate along q, as shown in Fig. 1.

Let us consider a simple two-dimensional case. The nematic director is in the (x, y) plane. An external dc electric field directed along the x axis is applied to the LC layer.

The photo-refractive-like bulk space-charge field, induced by charge separation, can be expressed as $E_{\rm ph} \sim \sin(q\xi)$,[14] with a symmetric line profile. As a result of the phase grating induced by these space-charge fields with a sinusoidal profile, the grating vector is pointing along ξ as shown in Fig. 6.

Zhang[15] predicted that only the surface-charge field contributes to the orientational photorefractive effect. To obtain the surface-charge field pattern, it is necessary to take into account the *y*-axis component. As shown in Fig. 6, it is obvious that the space-charge field profile along the *y* axis (the surface-charge field) becomes asymmetric. These asymmetric surface-charge fields, in conjunction with the applied dc field, cause a surface torque on the director axis *n*. These torques re-orient the director, leading to there being no sinusoidal refractive index grating. i.e., the dynamic phase grating.

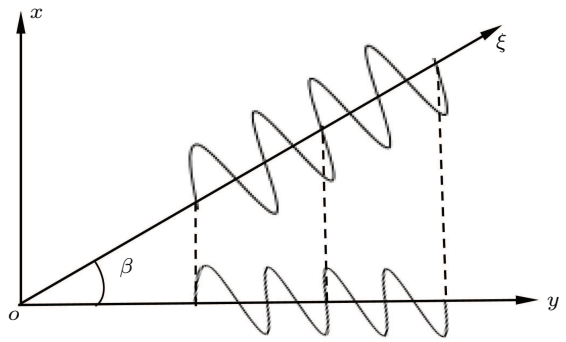


Fig. 6. (color online) Schematic representation of the surface-charge field with saw-tooth profile along the surface (*y*-axis component).

Based on the above analysis and recent publications,[16,17] we believe that the space-charge field profile is formed along the *y*-axis component with a saw-tooth profile as shown in Fig. 6. As a result, a saw-tooth profile phase grating with an asymmetric profile is developed. This assumption is confirmed by our experimental results.

Our work of these experimental findings may offer a new avenue for fabricating a phase grating with an asymmetric profile which is formed in the NLC. A model for the dynamic phase holographic grating, with the profile shape close to saw-tooth in NLC, is developed. However, the mechanisms responsible for the asymmetric surface-charge field, the shape of asymmetric grating, and the function of the asymmetric grating have not been fully understood yet. Therefore, further investigations are needed to clarify the mechanisms of the observed phenomena and more in-depth studies are needed to understand other unexplored effects.

4. Conclusions

In this paper, we presented a new method, for the first time, to fabricate a dynamic phase grating with an asymmetric profile in a C_{60}-doped homeotropically aligned nematic liquid crystal (NLC) under a dc voltage applied to the cell. The asymmetrization of the profile of a dynamic phase holographic grating on the basis of the photorefractive-like (PR) effect was proposed. The appearance of a dynamic asymmetric diffraction distribution and an increasing in the diffraction efficiency, up to 40% in one of these orders, can be explained by assuming that a grating with an asymmetry close to a saw-tooth profile is formed in the NLC.

We believe that the asymmetric dynamic phase holographic grating caused by the asymmetric surface-charge field and the Carr–Helfrich effect in the bulk, in conjunction with the applied dc field, causes a surface torque on the director axis *n*. The diffraction efficiency of the asymmetric dynamic grating can be controlled by applying a dc voltage. The investigation showed the possibility of automatic formation of an asymmetric phase profile, as a result of which the diffraction efficiency may exceed the theoretical limit for symmetric profile gratings. It should be noted that the unique optical properties of LC materials make it possible to use them in dynamic holography, which opens the way for creating new devices for optical information processing.

References

[1] Vasil'ev M V, Venediktov V Y and Leshchev A A 2001 *Quantum Electron.* **31** 1
[2] Venediktov V Y, Nevskaya G E and Tomilin M G 2011 *Opt. Spectrosc.* **111** 113
[3] Lan M and Ren C Y 2011 *Chinese Journal of Liquid Crystals and Displays* **26** 443
[4] Venediktov V Y 2012 *Optoelectronics, Instrumentation and Data Processing* **48** 126
[5] Shrestha P K, Chun Y T and Chu D 2015 *Light Sci. Appl.* **4** e259
[6] Magnusson R and Gaylord T K 1978 *J. Opt. Soc. Am.* **68** 806
[7] Venediktov V Y and Freigang N N 2008 *Opt. Spektrosk.* **104** 295
[8] Venediktov V Y, Laskin V A and Savinov V A 2010 *Opt. Spektrosk.* **109** 622
[9] Berenberg V A and Venediktov V Y 2001 *J. Opt. Technol.* **68** 665
[10] Venediktov V Y, Laskin V A, Pasechnik I M and Savinov V A 2010 *Opt. Spektrosk.* **109** 978
[11] Khoo I C 1994 *Opt. Lett.* **19** 1723
[12] Khoo I C 1996 *IEEE J. Quantum Electron.* **32** 525
[13] Zhang G Q, Montemezzani G and Gunter P 2000 *J. Appl. Phys.* **88** 1709
[14] Sun X, Ren C Y, Pei Y B and Yao F F 2008 *J. Phys. D* **41** 245105
[15] Zhang J, Ostroverkhov V and Singer K D 2000 *Opt. Lett.* **25** 414
[16] Berenberg V A and Venediktov V Y and Laskinb V A 2010 *Opt. Spectrosc.* **109** 966
[17] Venediktov V Y, Laskin V A, Pasechnik I M and Savinov V A 2010 *Opt. Spectrosc.* **109** 978